*Regular Article*

# Inducing aggresome and insoluble tau aggregation using an optogenetic tool

Shigeo Sakuragi[1], Tomoya Uchida[1#], Naoki Kato[1#], Boxiao Zhao[1], Akito Hattori[1$], Yoshihiro Sakata[1], Yoshiyuki Soeda[2], Akihiko Takashima[2], Hideaki Yoshimura[3], Gen Matsumoto[4], Hiroko Bannai[1*]

[1] *Department of Electrical Engineering and Biosciences, School of Advanced Science and Engineering, Waseda University, Shinjuku-Ku, Tokyo 162-0056, Japan.*

[2] *Laboratory for Alzheimer's Disease, Department of Life Science, Faculty of Science, Gakushuin University, Toshima-ku, Tokyo 171-8588, Japan*

[3] *Department of Chemistry, School of Science, The University of Tokyo, Tokyo 113-0033, Japan*

[4] *Department of Neurological Disease Control, Graduate School of Medicine, Osaka Metropolitan University, Osaka, 545-8585, Japan*

*# Equally contributed*

*$ Current affiliation： Department of Medical Laboratory Science, Kitasato University School of Health Sciences, Minami-Uonuma, 949-7241, Japan*

Received Month date, year; Accepted Month date, year;
Released online in J-STAGE as advance publication Month date, year
Edited by Editor Name

**Tauopathy is a group of diseases characterized by fibrillary tau aggregate formation in neurons and glial cells of the brain. Tau aggregation originates in the brainstem and entorhinal cortex and then spreads throughout the brain in Alzheimer's disease (AD), which is the most prevalent form of tauopathy. Understanding the mechanism by which locally formed tau pathology propagates throughout the brain is crucial for comprehending AD pathogenesis. Therefore, a novel model of tau pathology that artificially induces tau aggregation in targeted cells at specific times is essential. This study reports a novel optogenetic module, OptoTau, human tau with the P301L mutation fused with a photosensitive protein CRY2Olig, which induced various forms of tau according to the temporal pattern of blue light illumination pattern. Continuous blue light illumination for 12 h to Neuro2a cells stably expressing OptoTau (OptoTauKI cells) formed clusters along microtubules, many of which eventually accumulated in aggresomes.**

**Conversely, stable tau aggregates were formed when alternating light exposure and darkness in 30-min cycles for 8 sets per day were repeated over 8 days. Stable tau aggregates were induced more rapidly by repeating cycles of 5-min illumination followed by 25 min of darkness over 24 h. These results indicate that OptoTau induced various tau aggregation stages based on the temporal pattern of blue light exposure. Thus, this technique demonstrates potential as a novel approach to developing specific tau aggregation in targeted cells at desired time points.**

**Keywords:** Tauopathy, Alzheimer's disease, CRY2Olig

## ◀ *Significance* ▶

This study developed a technique to manipulate tau aggregation in a blue light-dependent manner using cells that stably express OptoTau, which is an optogenetic tool based on the CRY2Olig module. Tau accumulation in aggresomes or insoluble tau aggregation were specifically induced in response to blue light illumination conditions. These results are crucial as they provide a new technological basis for developing a singular point of tau aggregation in specific targeted cells at a specific time.

Corresponding author: Hiroko Bannai, School of Advanced Science and Engineering, Department of Electrical Engineering and Biosciences, Waseda University, 2-2 Wakamatsu-cho, Shinjuku-Ku, Tokyo 162-0056, Japan. ORCID iD: https://orcid.org/0000-0002-0951-488X e-mail: hiroko.bannai@waseda.jp

## Introduction

Tauopathy is a group of diseases that is characterized by neurofibrillary tangles (NFTs), which are filamentous tau protein aggregates that are formed in neurons and glial cells in the brain [1]. Tauopathy manifests as various disorders, such as Alzheimer's disease (AD), Pick's disease, progressive supranuclear palsy (PSP), corticobasal degeneration (CBD), and chronic traumatic encephalopathy (CTE), despite being triggered by abnormalities in the same molecule tau. Microtubule-binding protein tau in healthy neurons plays physiological roles, such as neurite outgrowth and axonal transport regulation by motor proteins. However, tau detaches from microtubules and forms intracellular tau aggregates when tau undergoes post-transcriptional modifications, including excessive phosphorylation [2]. The hyperphosphorylation of tau as a cause of NFT is initially formed in the neurons in locus coeruleus (LC) and entorhinal cortex (EC) in AD, which is the most prevalent form of tauopathy [3] [4]. This tau aggregation expands with age into the transentorhinal region, hippocampus, and cerebral cortex (temporal lobe, prefrontal cortex, and higher sensory association neocortex) [4]. Tau aggregation progression is closely associated with the clinical pathology development of AD [5] [6].

Several model experimental systems have contributed to understanding the association between degenerative tau accumulation and higher brain functions in AD and the mechanisms underlying tau pathology expansion. Tau aggregate formation, synapse loss, neurodegeneration, and brain atrophy have been observed in a few months in mice that overexpress neurons with human tau with the mutation in 301st proline to serine or leucine (P301S or P301L) found in familial frontotemporal dementia [7] [8] [9] [10]. These phenotypes demonstrate common pathologies in human patients; thus, these mice were selected as an AD model, helping elucidate the mechanism of toxicity from degenerated tau. Tau filaments polymerized *in vitro* and insoluble tau fractions from patients with AD injected into human tau-overexpressing mice form hyperphosphorylated tau and tau aggregates in distant brain regions with neuronal connections [11] [12] [13]. Additionally, tau extracted from patient brains induces pathology, even in non-transgenic mice [14] [15]. The spread of degenerated tau to healthy neurons has occurred through synaptic contact or by another cell uptake of degenerated tau that is extracellularly released dependent on a synaptic activity [16] [17]. These experiments have helped elucidate some aspects of tauopathy pathogenesis as model systems that rationally reproduce some of the phenotypes seen in AD and other tauopathies in humans.

Recently, Nagai et al. defined a "singularity phenomenon" as a biological phenomenon in which a small number of rare cells, named "singularity cells," significantly change a complex system [18] [19]. Therefore, neurons that first accumulate hyperphosphorylated tau and NFTs in LCs and ECs were regarded as "singularity cells" in AD [20]. Addressing the following questions is considered crucial for understanding the onset mechanisms of AD: "How do these 'singularity cells' initially accumulate tau arise?" and "How is tau degeneration transmitted from the singularity cells to the entire cortex?" However, to address this issue, the current experimental system of tauopathy models faces several challenges to overcome. Brain regions tend to aggregate tau, which is identified in tauopathy model mice with human tau overexpression, but the development of the first "singularity cells" that accumulate tau and their mechanism to produce tau aggregation remains unclear. More seriously, the loss of endogenous genes and uncertain protein expression levels of transduced tau in human tau overexpression model animals have been observed, and whether tau abnormalities cause the phenotypes obtained so far requires reconsideration [10]. Tau aggregation is another AD model, obtained by injecting exogenous tau seeds, and it bypasses the initial process of AD pathogenesis. Tau seed uptake is entirely random, and identifying the cell from which the pathology originates is impossible. A new model system is required to establish a singular point of tau aggregation at a targeted time in specifically targeted cells to elucidate the tau pathology process from the singularity cells, which are neurons that first develop tau pathology.

This study applied optogenetics to induce tau aggregation in targeted cells. CRY2, which is a photoreceptor in *Arabidopsis*, and its derivative CRY2Olig are optogenetic modules that reversibly form oligomers upon blue light exposure [21]. Recently, researchers have introduced CRY2 to induce protein aggregation in neurodegenerative diseases, including tau [22] [23] [24] [25] [26]. CRY2 and tau fusion proteins accumulated on microtubules by blue light illumination-induced liquid–liquid phase separation (LLPS) [23]. Blue light illumination forms tau droplets and oligomers in primary cortical culture neurons of mice that overexpress tau fused with CRY2Olig, which is a higher capacity for homo-oligomer formation [24]. We have recently revealed that "OptoTau," which is a fusion of human tau with the P301L mutation and CRY2Olig, is transiently overexpressed in Neuo2a cells and induced LLPS droplets and oligomers of tau by illuminating blue light for 24 h [25] [26]. The present study manipulated intracellular tau by blue light illumination in Neuro2a cells that stably express OptoTau. OptoTau, inserted into the safe-harbor region by CRISR/Cas9 technique, underwent various temporal patterns of blue light illumination, including eight-day illumination. Here, we report that different blue light illumination patterns enable the same optogenetic tool, OptoTau, to induce opposite responses: cell-protective response forming aggresome and toxic response forming insoluble tau aggregates.

## Materials and Methods

### OptoTau knock-in into Neuro2a cells

OptoTau consists of the optogenetic module CRY2Olig [21], a SNAP-tag, and a full-length human tau (2N4R) with a P301L (Figure 1A). ROSA26 MCS was used to develop the OptoTau-donor vector, OptoTau gene under the CMV promoter, and GFP and Puromycin-resistant genes under the EF1α promoter. Lipofectamine 3000 (Life Technologies) was used to transfect the OptoTau-donor and mROSA26sgRNA/Cas9 vectors (GeneCopoeia), including the guide RNA and Cas9 sequences, into mouse neuroblastoma-derived Neuro2a cells (JCRB Cell Bank). Drug selection was performed by adding 400 µg/ml of G418 (Nacalai tesque) on day one post-transfection and 1 µg/ml of puromycin (Nacalai tesque) after 4 days. GFP was used as a gene insertion marker, and GFP-positive cells were isolated into a 96-well plate. Single GFP-positive cell colonies were replated into a 24-well plate and further expanded on a 10-cm culture dish. This study used one clone as OptoTau knock-in (OptoTauKI) cells after confirming OptoTau expression.

### Cell Maintenance

OptoTauKI and Neuro2a wild type (WT) were maintained in Dulbecco's Modified Eagle's medium (4.5 g/l of glucose; Nacalai tesque) supplemented with 10% FBS, penicillin (100 units/ml), and streptomycin (100 µg/ml) mixture, in 5% $CO_2$ at 37°C environments. OptoTauKI cells were kept under light-shielded conditions to prevent irregular CRY2Olig conformational changes caused by room light. Cells were plated on a 35-mm glass bottom dish (MATSUNAMI) coated with 0.04% polyethyleneimine (PEI, Sigma-Aldrich) for the live imaging experiment. Cells were plated on an 18-mm cover glass precoated with 0.04% PEI for fixation. The density of light-exposed cells was always maintained at 60%–80% confluence, except in the experiment where the cells were incubated for 48–72 h after light illumination.

### Blue light illumination

A blue light illumination device (TH2-211X200BL, CCS Inc.) was set in a 5% $CO_2$ incubator at 37°C. Plates of cells were placed on a transparent plastic box with a 30-mm height on the light-emitting device. The light intensity was 0.24 ± 0.04 mW/cm$^2$ throughout all experiments. This study performed the illumination protocol, one 12-h illumination, 8 cycles of 30-min illumination of 30-min light off per day for up to 8 days, and 48 cycles of 5-min illumination at 25-min light off per day. An automatic timer controlled the illumination timing.

### Labeling of OptoTau using SNAP-tag

Fluorescent labeling of OptoTau molecules was performed by covalently binding a fluorescent-labeled SNAP ligand to a SNAP tag inserted into the OptoTau. SNAP-Cell 647-SiR (New England BioLabs) of 0.1 µM was administered into the culture medium, and OptoTau KI or WT was applied for 12–18 h. Cells were washed with medium and then used for live cell imaging or immunocytochemistry.

### Immunocytochemistry

Phosphate buffered saline (PBS) was used for dilution and washing throughout the immunocytochemistry. Cells were generally fixed with 4% paraformaldehyde (PFA) for 15 min at room temperature (RT: ~24°C) and permeabilized with 0.1% Triton X-100 for 3 min at RT. Cells were fixed with ice-cold acetone/methanol (acetone: methanol = 1:1) for 3 min at −20°C, followed by post-fixation with 4% PFA (15 min, RT), for immunostaining of microtubule or aggresomal markers. Cells were fixed with ice-cold methanol for 20 min at −20°C to visualize insoluble tau. This treatment removes soluble tau in the cytosol [27]. Cells were incubated with 5% bovine serum albumin (BSA) for 30 min at RT for blocking after fixation and permeabilization, then with primary antibody treatment in 2.5% BSA for 1 h at RT. Primary antibodies used were anti-total tau antibody (RTM38, 1:1000, Fujifilm), an antibody recognizing the initial structural change of pathological tau (MC1, 1:1000; gifted from Prof. Peter Davies [Albert Einstein College of Medicine Medicine]), anti-αTubulin antibody (1:2000; Sigma-Aldrich), anti-γTubulin antibody (1:100; Santa Cruz), anti-HDAC6 antibody (1:100; Santa Cruz), and anti-Dynein antibody (1: 100; Santa Cruz). Cells were incubated with secondary antibodies after washing with PBS (5 µg/ml in 2.5% BSA) for 40 min at RT. Secondary antibodies used were anti-rat IgG (H + L) Alexa Fluor® 555 conjugate, anti-rat IgG (H + L) Alexa Fluor® 647 conjugate (Cell signaling) or goat anti-Rat IgG (H + L) cross-adsorbed secondary antibody (Alexa Fluor™ 594), goat anti-Mouse IgG (H + L) cross-adsorbed secondary antibody (Alexa Fluor™ 647), and goat anti-mouse IgG (H + L) cross-adsorbed secondary antibody (Alexa Fluor™ 555) (Thermo Fisher Scientific).

### Observation by epifluorescence and confocal laser scanning microscopies

An inverted microscope (IX73; Evident) equipped with a high-intensity LED driver (DC4104, Thorlabs) and a digital CMOS camera (ORCA-Fish 4.0; HAMAMATSU) was used to observe immunocytochemically or SNAP-tagged cells, set at 60× oil immersion objective (NA 1.42; Evident), 1.6× optical zoom, and 5–10 fields of view captured from a

single cover glass. Confocal laser scanning microscope (FV3000; Evident) images were taken with an oil immersion objective (×60, NA1.42; Evident) at 5× digital zoom.

**Image Analysis**

MetaMorph (Molecular Devices) or ImageJ (NIH) image analysis software was used to contrast-adjust epifluorescence or confocal microscopy images. The percentage of cells with insoluble tau aggregates in the field of view was calculated per images of PFA-fixed samples. The greater maximum RTM38 intensity value in the cell than "the mean of the RTM38 intensity + 3 standard deviation" of the dark condition indicates the presence of the aggregates. The presence of aggregates around the nucleus was measured at the focal plane, where the nucleus was maximally visible and calculated as a percentage per coverslip.

**Western blotting**

Immediately after completing blue light illumination, $2.0 \times 10^6$ cells/mL of WT Neuro2a or OptoTau KI cells were incubated in 10 mM of HEPES buffer supplemented with 1% protease inhibitor (cOmplete, Roche), 1 μM of okadaic acid (Cayman Chemical), 1 mM of sodium orthovanadate (MP Biomedicals), 1 mM of sodium fluoride (Nacalai tesque), 1 mM of β-glycerophosphate disodium salt hydrate (Sigma–Aldrich), 250 mM of sucrose, and 1 mM of ethylenediaminetetraacetic acid. Samples were subjected to 15 s of sonication followed by 15 s of ice-cooling 4 times and centrifuged at 3000 x g for 10 min at 4°C. The supernatant was mixed with non-reducing Tris-Glycine SDS sample buffer (TEFCO) and was loaded onto a 5%–20% gradient gel. Samples were electrophoresed at 40 mA and transferred to a polyvinylidene fluoride membrane (Bio-Rad). After transfer, the membrane was blocked with 1% BSA with 0.05% Tween-20 and reacted with an anti-tau antibody (RTM38, 1:2500) and anti-β-actin antibody (1:10,000; Sigma-Aldrich) at RT for 1 h (or 4°C O/N). After washing three times with PBST (0.05% Tween20 in PBS), the membrane was incubated with the secondary antibodies conjugated with peroxidase (1:10,000, Jackson Immuno Research) at RT for 1 h. A luminol-based chemiluminescence assay kit (Chemi-Lumi One L, Nacalai tesque) and chemiluminescence detection system (ChemiDoc Touch MP imaging system, Bio-Rad) were used to detect chemiluminescence signals.

**Statistics**

The numbers of data are indicated in the Figure legends. The Mann–Whitney U test was used to compare Western blots with and without blue light illumination and the percentage of cells with insoluble tau aggregates. Student's *t*-test was used to compare the percentage of tau aggregates in the perinuclear region for each light exposure pattern. The *p*-values in each figure are as follows: NS: $p > 0.1$, *: $p < 0.05$, ***: $p < 0.001$, ****: $p < 0.0001$.

**Results**

**Establishment of OptoTau knock-in (OptoTauKI) cells**

OptoTau is a protein fused to CRY2Olig [21], which forms multimeric complexes when exposed to blue light, with human 2N4R tau carrying the P301L mutation (Figure 1A). We have previously revealed that transient overexpression of OptoTau into Neuro2a and blue light exposure induced tau clustering [25] [26]. This study established Neuro2a cells that stably express OptoTau and investigated the effects of blue light illumination over a longer period than in previous studies. The CRISPR/Cas9 system was used to introduce OptoTau into the mouse Safe Harbor ROSA26 region. We designed the cells to express OptoTau under the CMV promoter and GFP for screening under the EF1α promoter (Figure 1A). We isolated GFP-positive single colonies and defined them as OptoTau knock-in (OptoTauKI) cells. We performed fluorescent labeling of SNAP-tag incorporated into OptoTau to confirm OptoTau expression and localization. Both GFP and SNAP647 labeling demonstrated no signal in non-genome-edited Neuro2a cells (WT), whereas GFP was observed throughout the OptoTauKI cells, and SNAP-tag signal was observed in the cytoplasm (Figure 1B). Live cell imaging with a confocal microscope demonstrated localized OptoTau in the cytoplasm, avoiding the nucleus (Figure 1C). These results indicate that OptoTau is inserted in OptoTauKI cells and that the expressed OptoTau resides mainly in the cytoplasm.

**Filament-like cluster formation of tau by 12-h blue light exposure**

We then examined the behavior of OptoTau in OptoTauKI cells under blue light illumination. OptoTauKI cells were continuously exposed to blue light for 12 h using a blue LED in a $CO_2$ incubator, then tau localization by SNAP staining or immunofluorescence staining. Both the SNAP signal and the signal of total tau visualized by the RTM38 antibody demonstrate uniform distribution in the cytoplasm in OptoTauKI cells cultured in the dark (Figure 2A, Dark). In contrast, OptoTau labeled with SNAP647 in OptoTau cells exposed to blue light for 12 h formed thick filament-like structures, also recognized by RTM38 antibody (Figure 2A, 12 h blue light).

Single-molecule localization microscopy has revealed that tau forms oligomers on microtubules [28]. We

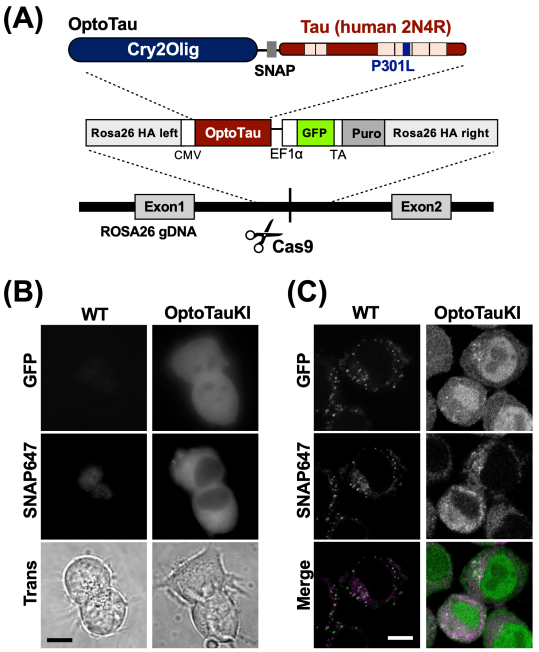


**Figure 1 OptoTau knock-in Neuro2a cells.**
(A)Top: Design of OptoTau, consisting of CRY2Olig, SNAP-tag, and human2N4R tau with P301L mutation; bottom: conceptual diagram of OptoTau knock-in to mouse ROSA26 locus using CRISPR/Cas9 system. The donor vector contains OptoTau expressed under the CMV promoter and GFP and Puromycin (Puro) sequences for screening. (B) Live cell imaging of GFP and SNAP647 fluorescence in Neuro2a cells (WT) and OptoTau knock-in Neuro2a cells (OptoTauKI). The SNAP647 signal reflects OptoTau localization. Transmission images (Trans) were obtained from the same field of view. Bar = 10 µm. (C) Confocal images of GFP and SNAP647 fluorescence in Neuro2a cells (WT) and Neuro2a cells knocking in OptoTau knock-in (OptoTau). Cells were fixed with 4% PFA. Bar = 10 µm.

performed multicolor immunofluorescence staining of tau and microtubules in the same cells to determine whether the filamentous tau formed by blue light illumination co-localizes with microtubules. OptoTauKI cells illuminated with blue light for 12 h were fixed with acetone methanol, and microtubules were labeled with α-tubulin antibody and tau with RTM38 antibody (Figure 2B). The filamentous tau signal largely colocalized with that of α-tubulin (Figure 2B, Merge).

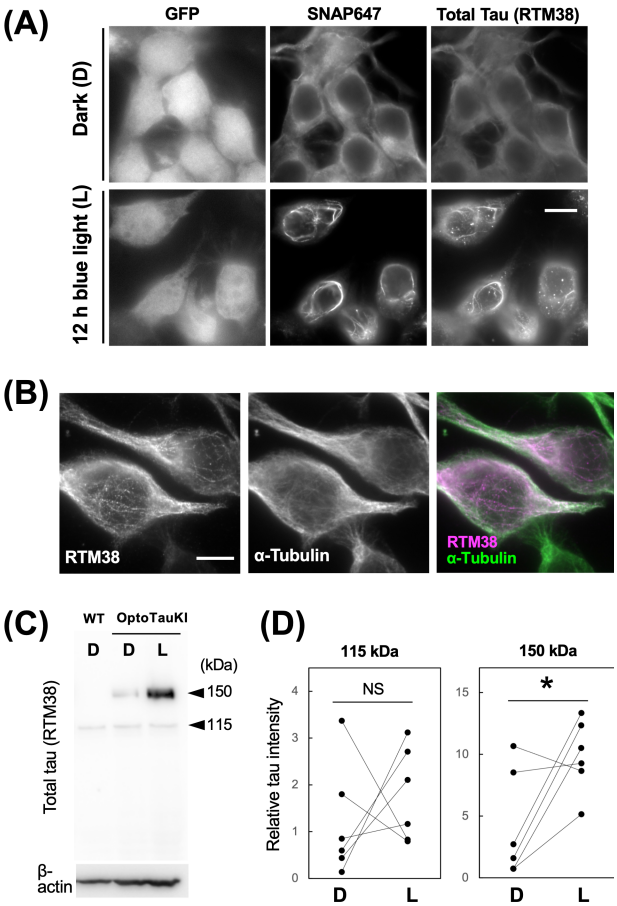


**Figure 2 Effect of 12 hours of blue light illumination on Tau in OptoTau knock-in cells.**
(A) Subcellular localization of GFP (left), OptoTau (middle, SNAP647), and total tau shown by immunofluorescence staining with RTM38 antibody in OptoTau knock-in cells. Top: cells kept in the dark condition (Dark [D]); bottom: cells fixed immediately after 12-h blue light (12 h blue light [L]). Scale bar = 10 µm. (B) Immunofluorescence staining images of microtubules (middle, α-tubulin) and total tau (left, RTM38) in OptoTauKI cells immediately 12 h after blue light illumination. The right panel demonstrates the merge of these signals (a-tubulin [green], total Tau [magenta]). Scale bar = 10 µm. (C) Western blotting analysis of Tau using RTM38 antibody in Neuro2a cells (WT) and OptoTauKI cells (OptoTauKI). D: Cells under dark; L: cells illuminated with blue light for 12 h. Bands of 151 kDa and 115 kDa were detected. β-actin was used as a loading control. (D) Quantification of 115 kDa (left) and 151 kDa (right) tau. The ratio of β-actin-normalized tau band intensity to that of Neuro2a cells (WT) was defined as relative tau intensity. D: under dark, L: 12-h blue light exposure. NS: $p > 0.1$, *: $p < 0.05$, Mann–Whitney U-test.

Furthermore, a Western blot using RTM38 antibody was used to confirm the tau expression level in OptoTauKI cells. Only a 115 kDa band was detected in Neuro2a cells (WT), whereas two bands of 115 kDa and 150 kDa were detected in OptoTauKI cells (OptoTau) with or without blue light exposure. The 115 kDa band can be interpreted based on the molecular weights as the tau dimer and the 150 kDa band as the OptoTau, conjugation of Cry2Olig, SNAP, and tau. The intensity of the 115 kDa and 150 kDa bands was quantified to investigate the changes in the amount of OptoTau protein with or without blue light illumination. Band intensities were normalized by β-actin, a loading control, and calculated as "relative tau intensity" relative to the value of Neuro2a cells (WT). The relative tau intensity of the 115 kDa band was not different between the cells with and without 12-h blue light exposure (Figure 2D, 115 kDa), whereas the relative tau intensity of the 150 kDa band was higher in the blue light group in 5 out of the 6 samples. These results indicate the increased amount of OptoTau protein in OptoTauKI cells by the 12-h blue light illumination.

**Tau dynamics in OptoTauKI cells after blue light illumination termination**

A 12-h blue light irradiation induced filament-like structures in OptoTauKI cells (Figures 2A and B). Concurrently, Western Blot detected no tau aggregates with large molecular weights, which could be oligomers (Figure 2C). Cells were fixed at 12, 24, 48, and 72 h after blue light termination to examine the stability of filamentous tau formed after the 12-h blue light illumination. The subcellular localization of tau and microtubules was investigated by immunofluorescence staining (Figure 3A). Filament-like tau co-localized with microtubules in OptoTauKI cells immediately after blue light termination, revealing a strong signal in part of them (Figure 3B, 0 h, arrowheads). A bright spot with dense tau was formed in the vicinity of the nucleus 24 h after blue light termination (Figure 3B, 24 h, arrows). Bright spots remained at 48 and 72 h, but the tau bright spot was fragmented in most cells. These results indicate that the filamentous tau formed in OptoTauKI cells after 12 h of blue light illumination is not a stable structure but an unstable one that can dynamically change morphology over time.

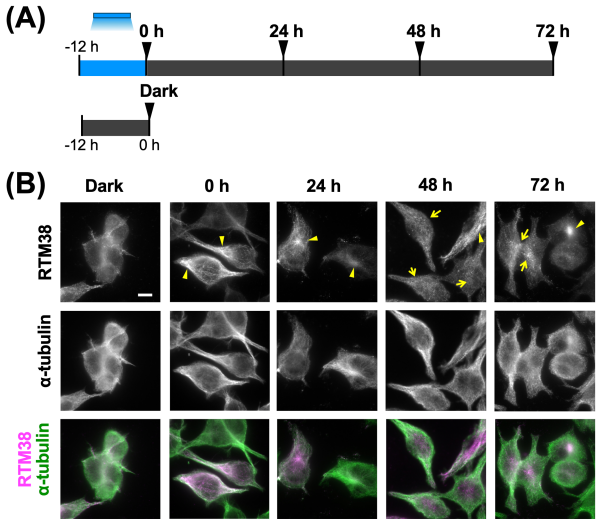


**Figure 3 Localization change of Tau after blue light illumination termination.**
(A) Schematic illustration of the experimental design. Top: Localization of total tau in OptoTauKI cells cultured in the dark after the 12-h of blue light illumination verified by immunofluorescence staining with the RTM38 antibody; the arrowhead indicates the timing of cell fixation. Dark demonstrates cells cultured in the dark for 12 h. (B) Immunofluorescence images of total tau and microtubules immediately (0 h), 24 h, 48 h, and 72 h after blue light exposure termination. Top: RTM38 antibody, middle: α-tubulin antibody, bottom: merge image. Yellow arrowheads indicate large bright spots of tau; arrows indicate fragmented bright spots of tau. Scale bar = 10 μm.

**Co-localization of tau with aggresome markers after blue light illumination**

Proteasome inhibition and uptake of tau-paired helical protofilaments from patients with AD have induced aggresomes, inclusion bodies for misfolded proteins [29] [30]. Aggresomes are formed in the microtubule organizing center (MTOC) located in the vicinity of the nucleus [31]. We performed immunofluorescence staining for γ-tubulin in the MTOC, together with tau, to investigate the possibility that the perinuclear tau accumulation in OptoTauKI cells after a 12-h blue light exposure is an aggresome. The tau accumulation in the vicinity of the nucleus observed immediately (0 h) and 24 h (24 h) after blue light termination was co-localized with γ-tubulin in MTOCs (Figure 4A, arrowheads). This result indicates the MTOC as the site of tau accumulation after blue light termination.

The process of transporting degenerated proteins along the microtube to the aggresome at MTOCs involves the microtubule motor protein dynein and histone deacetylase 6 (HDAC6), which recruits denatured proteins to dynein [32]. We investigated the co-localization of these aggresome marker proteins with tau to investigate the possibility that the solid bright spots of tau that appeared in OptoTauKI cells after blue light arrest were contained in aggresome and its precursors. Tau signal co-localized with HDAC6 and dynein in the near-nuclear bright spots (arrowheads) and thick filaments (Figures 4B and C, 0 h). Tau demonstrated stronger co-localization with HDAC6, or dynein, near the nucleus and in the cytoplasm 24 h after blue light termination. These results indicate that tau proteins are recruited to

aggresome-associated proteins and ultimately accumulated to the aggresome in OptoTauKI cells with 12-h continuous blue light exposure.

Western blot experiments revealed an increase in OptoTau of 150 kDa after 12 h of illumination (Figure 2D). RTM38 antibody immunostaining revealed cells with increased tau after 12 h of light exposure compared to dark conditions (Figure 4D, top). Interestingly, cells with increased tau upon light illumination exhibited increased HDAC6 protein levels (Figure 4D, bottom). This result indicates that the increase in tau levels and filamentous tau induced by light stimulation may activate aggresome formation.

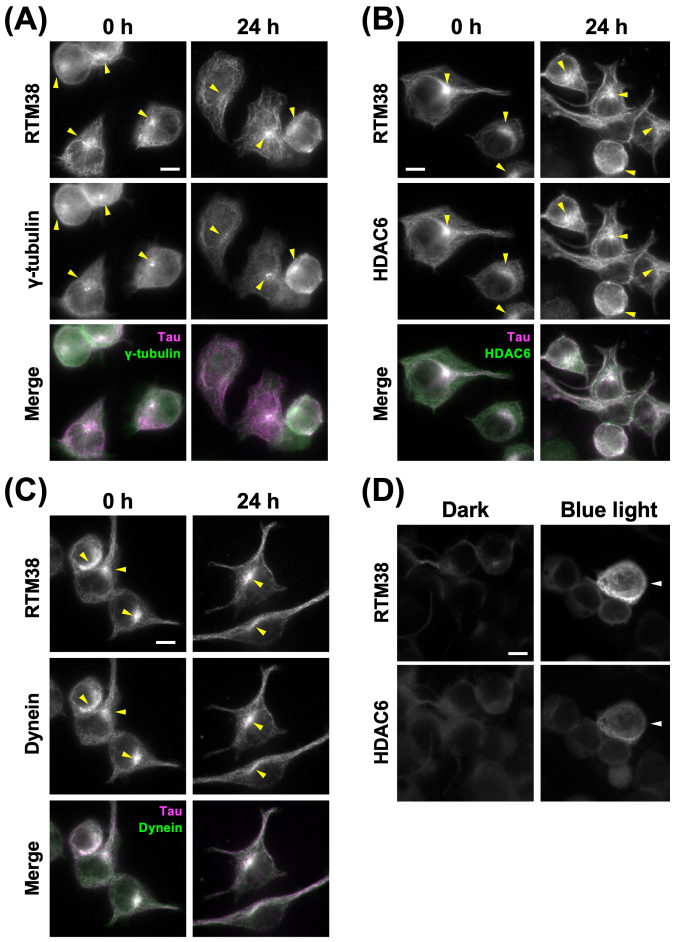


**Figure 4 Co-localization of tau with aggresome proteins after blue light illumination termination.**
Multicolor immunofluorescence images of tau and aggresomal proteins in OptoTauKI cells immediately (0 h) and 24 h after terminating 12-h blue light illumination. Aggresomal proteins labeled were (A) γ-tubulin, (B) HDAC6, and (C) Dynein. Yellow arrowheads exhibit strong bright spots of tau. (D) Tau (RTM38, top) and HDAC6 (bottom) immunostaining under dark conditions (Dark, left) and immediately after 12 h of blue light exposure (Blue light, right). The white arrowhead indicates a cell with high level of Tau expression. Scale Bars = 10 μm.

**Insoluble tau aggregation induced by intermittent blue light illumination**

Continuous blue light irradiation for 12 h induced tau translocation to the aggresome, where denatured proteins accumulated but did not form stable aggregates, as seen in AD and other tauopathy. We then searched for conditions that would induce stable tau aggregation in OptoTauKI cells. We expected repeated cluster formation and dissociation of OptoTau would be effective in increasing the probability of tau molecules interacting in an optimal position. Taking advantage of the 23.1 min half-life for CRY2Olig cluster dissociation [21], we established an illumination cycle in which a 30-min blue light exposure is followed by a 30-min dark period during which the CRY2Olig interactions are lost (Figure 5A). OptoTauKI cells express the OptoTau protein stably, enabling prolonged blue light illumination, which was impossible in transfected cells in previous studies. Therefore, we performed a 24-h illumination sequence consisting of a 16-h dark period followed by eight 30-min dark/30-min blue light cycles (repeated illumination), which was continued for 6–8 days (Figure 5A). The stability of the tau aggregation-like structures induced by blue light was assessed based on their presence 16 h after illumination termination.

Total tau labeled with RTM38 antibody demonstrated a thick linear filament structure immediately after repeated illumination for 6 and 8 days (Figure 5B, RTM38). This filament structure was not seen in OptoKI cells with a 6-day illumination cycle plus 16 h of darkness but remained in cells with an 8-day illumination cycle plus 16 h of darkness. The MC1 antibody is an antibody that recognizes the initial pathological tau conformation [33] [34]. Additionally, the MC1 antibody recognized the filament-like conformation immediately after terminating repeated illumination and after

16 h of illumination cycle for 8 days (Figure 5B, MC1), as did the RTM38 antibody. The percentage of cells with bright solid spots exhibiting stable tau aggregation 16 h after terminating repeated illumination was significantly higher after 8 days of illumination than after 6 days (Figure 5C).

Considering the effect of methanol fixation on removing soluble tau in the cytoplasm [27], we assessed insoluble tau formation by repeated illumination of OptoTauKI cells. Methanol-fixed cells immediately after 6 days of repeated irradiation demonstrated RTM38-positive aggregation in the cytoplasm, but this aggregation disappeared after16 h later (Figure 5D, Top). The amount of tau remaining after methanol fixation was increased immediately after 8 days compared to after 6 days of illumination and was detected as thick filament structures (Figure 5D, 8 days). This filament-like tau remained after 16 h (Figure 5D, 8 days + 16 h). The results indicate that repeated blue light exposure and dark incubation over 8 days generated stable tau aggregation.

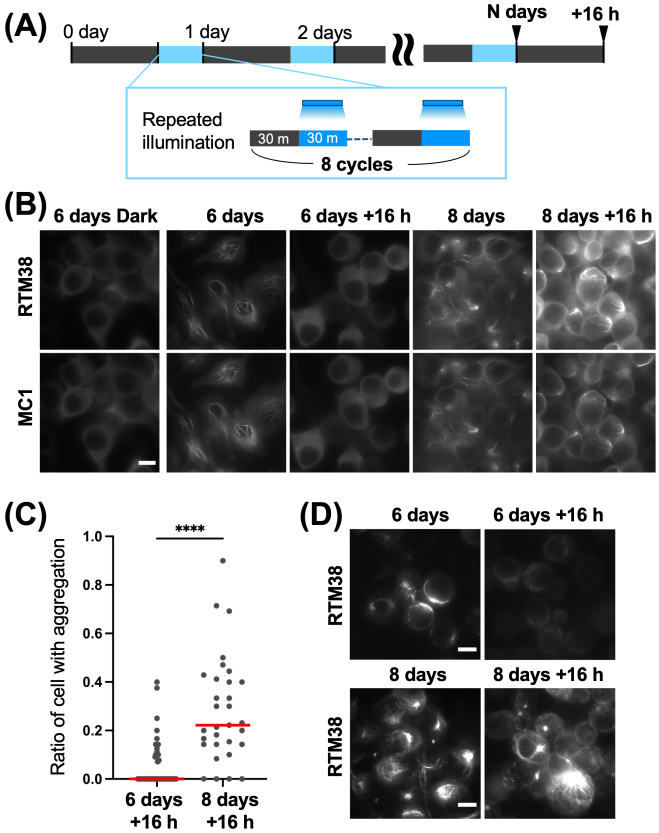


**Figure 5 Formation of insoluble tau aggregates by repeated blue light illumination.**
(A) Protocol for repeated blue light stimulation. OptoTauKI cells were cultured in darkness for 16 h, followed by 8 cycles of 30-min darkness/30-min blue light illumination, repeated for N days. Arrows indicate the timing of fixation. (B) Immunofluorescence staining using total tau antibody (RTM38) and tau conformation change recognition antibody (MC1) in OptoTauKI cells after repeated blue light stimulation. Cells cultured in the dark for 6 days (6 days Dark), cells fixed immediately after repeated blue light stimulation on 6 days (6 days), cells fixed at 16 h after 6 days of light stimulation (6 days + 16 h), cells fixed immediately after repeated blue light stimulation on 8 days (8 days), cells fixed at 16 h after 8 days of light stimulation (8 days + 16 h). Scale bar = 10 µm. (C) Percentage of cells with insoluble tau aggregation 16 h after repeated blue light exposure. The red lines indicate the median. 6 days + 16 h: N = 46 images; 8 days + 16 h: N = 31 images. ****: $p < 0.0001$, Mann–Whitney U-Test. (D) Visualization of intracellular insoluble Tau by methanol fixation at 6 days and 6 days + 16 h (top), 8 days and 8 days + 16 h (bottom), using RTM38 antibody. Scale bar = 10 µm.

**Acceleration of insoluble tau aggregation formation by short light-dark cycles**

Finally, we investigated the association of the temporal pattern of blue light/dark cycle repetitions with the time to induce insoluble tau aggregation. Here, 25 min of dark/5 min blue light illumination cycles were repeated 48 times (Figure 6A). The total required time was 24 h, with a total illumination time of 4 h. A 25-min dark/5-min blue light cycle for 24 h formed thick tau filaments as detected by RTM38 and MC1 antibodies (Figure 6B, left). MC1-positive tau filaments remained after 16 h of dark incubation after the illumination cycle (Figure 6B, right). The immunofluorescent staining after methanol fixation confirmed the stability of filamentous tau in OptoTauKI cells immediately after the end of the cycle and after 16 h of dark incubation after the cycle (Figure 6C). These results indicate that insoluble tau could be induced in only 24 h by repeating the 25-min dark/5-min blue light exposure cycle. The same 48 cycles of light illumination did not induce stable tau aggregation when 8 set cycles of 30-min dark/30-min blue light were repeated for 6 days (Figure 5); despite the longer duration of each illumination (30 min vs. 5 min), total illumination time (24 h vs. 4 h), and total time required (6 days vs. 1 day). Furthermore, fibrous tau aggregation was hardly formed by 144 cycles of 1-min blue light/9-min dark illumination, despite the high number of cycles (data not shown). The results indicate that the temporal pattern, including the duration of one illumination, interval time, and number of repetitions, must be appropriately set to introduce insoluble aggregation with OptoTau.

Interestingly, insoluble tau aggregates induced by the 5-min light/25-min dark cycle were less frequently located near the nucleus where aggresomes were formed (Figure 4). An average of 69.64 ± 2.90% (n = 9) of the tau aggregates

were located in the nuclear vicinity in OptoTauKI cells illuminated continuously for 12 h, by which tau accumulation in the aggresome was observed. Conversely, significantly less tau aggregation was found in the vicinity of the nucleus in cells illuminated for 24 h with 5-min light/25-min dark cycles (34.54 ± 4.06% [n = 6]) (Figure 6D, $p < 0.001$, student's *t*-test). This result indicates that the insoluble tau induced by the 5-min blue light/25-min dark cycle escaped translocation to aggresomes.

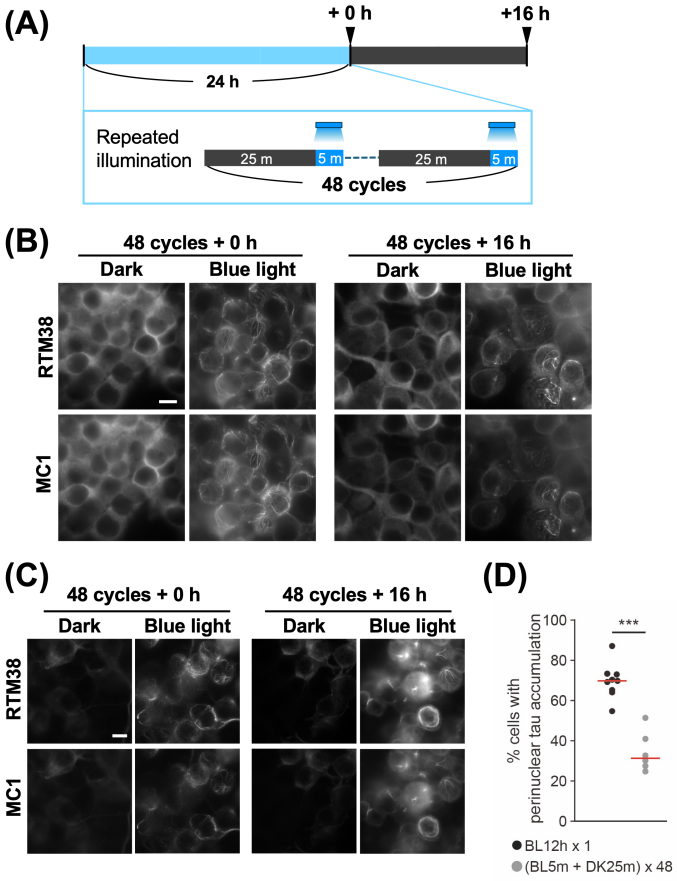


**Figure 6 Acceleration of insoluble tau aggregation formation by repeated blue light illumination.**
(A) Protocol for repeated blue light stimulation. The cycle was repeated for 48 consecutive cycles (24 h), each cycle consisting of 25 min of darkness and 5 min of blue light illumination. Arrows indicate the timing of fixation. (B) Immunofluorescence staining using RTM38 and MC1 in OptoTauKI cells after repeated blue light stimulation. PFA fixation was performed immediately after the end of 48 cycles (48 cycles + 0 h) or 16 h after the end of 48 cycles (48 cycles + 16 h) in the blue light (Blue light) and dark conditions (Dark), respectively. (C) Intracellular insoluble Tau by methanol fixation, immediately after the end of 48 cycles (48 cycles + 0 h) or 16 h after the end of 48 cycles (48 cycles + 16 h) in the blue light (Blue light) and dark conditions (Dark), respectively. (D) Comparison of the percentage of cells with perinuclear tau accumulation of the single 12-h blue light illumination (BL 12 h × 1) and the 48 repetitions of 25-min off/5-min blue light illumination ([BL 5 m + DK 25 m] × 1]. Fixation was performed immediately after completing the total blue light illumination program in both groups. The red lines indicate the median. BL 12 h × 1: N = 9 coverslips; (BL 5 m + DK 25 m) × 48: N = 6 coverslips. ***: $p < 0.001$, Student's *t*-test. Scale bars = 10 µm.

## Discussion

The present study generated cells knocking in OptoTau, an optogenetic tool based on the CRY2Olig module, and developed a technique to manipulate tau aggregation with blue light. We discovered light illumination conditions that specifically induce tau accumulation in aggresomes or insoluble tau aggregation.

Recently, a series of studies revealed that transient overexpression of chimeric proteins combining tau with Cry2 or its derivative CRY2Olig, i.e., families of OptoTau, results in the blue light-dependent formation of LLPS droplets and tau oligomers [23] [24] [25] [26]. The present study manipulated tau by blue light in OptoTauKI cells, in which OptoTau was inserted into the genome by genome editing. The transfected plasmid is diluted by cell division in dividing cells, thereby attenuating the expression level of the product. Here, using a cell line that stably expresses OptoTau allowed us to validate the blue light illumination protocol over several days while maintaining OptoTau expression.

A previous study showed that tau condensate formed along microtubules within 50 s when SH-SY5Y and HeLa cells overexpressing Cry2WT-mCherry-tau, a protein fusing CRY2 and human wild-type tau in a previous study, were exposed to blue light [23]. Consistent with this study, here we found that tau formed filament structures colocalizing with microtubules in OptoTauKI cells exposed to blue light for 12 h. Conversely, blue light exposure for 3 min to primary cortical culture neurons overexpressing Tau::CRY2, which is CRY2Olig fused to the C-terminus of human

wild-type tau, induced tau droplets and oligomers [24]. Such a tau droplet, which is considered an LLPS droplet, was induced by 24-h blue light illumination in the presence of microtubule depolymerizing agent nocodazole in Neuro2a cells overexpressing our OptoTau, consisting of CRY2Olig-SNAP-human tau with P301L [25]. However, the present no droplet-like structures induced in OptoTauKI cells by any light illumination protocols. The differences in the OptoTau complex morphology induced by blue light may depend on multiple parameters, including the expression levels of OptoTau, cellular endogenous tau, blue light exposure time, exposure intensity, cell type, and microtubule integrity.

Some filamentous tau induced by 12-h blue light illumination on OptoTauKI accumulated in MTOCs stained with γ-tubulin and co-localized with HDAC6 and dynein, both component proteins of aggresomes. OptoTau accumulation in aggresomes was also observed in Neuro2a cells overexpressing OptoTau [25]. The increased HDAC6 amount in cells with elevated tau content implies that selective autophagy is triggered as a stress response. Our study did not confirm tau ubiquitination up-regulation, which is a signal for transport to aggresome. Additionally, increased aggresome activity after light stimulation, causing OptoTau and endogenous tau degradation, remains unclear. Previous studies revealed increased phosphorylated tau and tau oligomers in the hippocampus of mice in which the aggresomal protein p62 is knocked out [35]. Optogenetically accumulated OptoTau co-localizes with endogenous p62 [25]. The role of p62 in light-induced aggresome formation and tau degradation warrants further verification.

This study revealed two illumination conditions that induce methanol-fixation-resistant tau aggregation: one is to repeat a 24-h illumination sequence consisting of a 16-h dark period followed by eight 30-min dark/30-min blue light cycles for 8 days, and another is repeating 25-min dark/5-min blue light cycles for 24 h. This aggregation did not disappear even 16 h after light illumination termination. Therefore, these tau aggregates are interpreted as a stable residual structure. Initial conformational changes in pathological tau labeled by the MC1 antibody were detected even before stable aggregation was generated but only remained when tau aggregation was present after methanol fixation. A previous study revealed that OptoTau with the truncated N-terminal of tau optogenetically induced sarcosyl-insoluble tau aggregation, while OptoTau with full-length tau did not induce insoluble tau aggregation [25]. The N-terminal of tau inhibits full-length tau polymerization [36]; thus, OptoTau lacking its N terminal is more likely to produce aggregation seed. The present study indicates that even full-length tau could be transformed into stable aggregation by light illumination with repeated on/off cycles. Opto-α-synuclein, which is α-synuclein fused with CRY2Olig, was induced to form stable aggregates in human iPS cell-derived neurons by repeated stimulation at 0.17 Hz. Repeated on/off stimulation and periods of no light exposure are effective means of avoiding phototoxicity. Additionally, the CRY2Olig module may be repeatedly stimulated to induce stable aggregation. In particular, OptoTau is a microtubule-binding protein that can be trapped in microtubules, making it difficult to interact with each other at optimal positions. The frequent OptoTau concentration by blue light followed by dissociation during the dark period may increase the possibility of interaction between tau molecules at appropriate positions. Stable aggregation could be induced in a shorter period (8 days to 1 day) despite the shorter total time of blue light illumination (24 hours to 4 hours) by accelerating the light illumination cycles. This result indicates that tau aggregation can be induced more efficiently when CRY2Olig binding/dissociation is repeated rapidly. This study only demonstrated two conditions under which stable tau aggregation induction is possible, and the optimal aggregation induction system should be further explored.

This study demonstrated that OptoTau induces opposing behaviors such as aggresome formations and stable tau aggregation, i.e., proteolysis and protein aggregation, depending on the temporal pattern of the light stimulation. OptoTau presents a new experimental possibility for future introduction into the mouse brain, where the assembly state of tau can be manipulated with light at the intended timing in specific cells at the targeted brain region. Additionally, this optogenetic tool could help validate the existence of "singularity cells," i.e., a small number of rare cells that cause significant changes throughout the system [18]. The neurons that first form tau aggregates in LCs and ECs can be assumed to be "singularity cells" in AD [20]. OptoTau that specifically induces tau aggregation only in LCs and ECs will verify whether they can be "singularity cells" that spread tau pathology to the cortex.

Some issues warrant resolution before using OptoTau as a model for tauopathies in the future. One is the isoform of tau. The tau isoform with the 31 amino acid repeats encoded by exon 10 is named the 4R isoform, and the isoform without the repeats is called the 3R. The tau aggregates of AD and CTE contain 3R and 4R tau, whereas Pick's disease is composed of only 3R tau, and CBD and PSP are composed of only 4R tau. The molecular structure of the filaments within tau aggregates varies in each tauopathic disease [10]. The molecular structure of the tau aggregation core determines the tau aggregate properties (including the 3R tau to 4R tau ratio) specific to tauopathies [37]. Current OptoTau includes only 4R-type tau. In the future, developing 3R-type OptoTau will be necessary to create optogenetic models specific to AD, CTE, and Pick's disease. The 3R to 4R tau expression ratio in OptoTau-induced cells should be controlled. Additionally, optogenetically inducing aggregation nuclei specific to each tauopathy will be a significant challenge.

## Conclusion

This study utilized the optogenetic tool OptoTau, based on the CRY2Olig module, to induce tau aggregation in cells. Specific light exposure conditions introduced aggresome and insoluble aggregation in OptoTauKI cells. The present results will provide a new technological basis for establishing a singular point of tau aggregation at a targeted time in targeted cells.

## Conflict of Interest

The authors have no conflict of interest related to this publication.

## Author Contributions

SS, TU, NK, BX, AH, and YS performed the experiment. SY, AT, HY, GM, and HB were involved in the design and supervision of this work. SS, TU, NK, BX, AH, and HB processed the experimental data, performed the analysis, drafted the manuscript, and designed the figures. All authors discussed the results and commented on the manuscript.

## Data Availability

The evidence data generated and/or analyzed during the current study are available from the corresponding author upon reasonable request.

A preliminary version of this work, DOI: https://doi.org/10.1101/2024.05.07.592868, was deposited in the bioRxiv on May 8th, 2024.

## Acknowledgments

The authors thank Prof. Peter Davies (Albert Einstein College of Medicine) for providing the MC1 antibody, Dr Sumiyo Mimura (AS ONE Corporation) for technical support of single cell cloning, and Dr. Naruhiko Sahara (National Institutes for Quantum Science and Technology) for insightful discussion. This research was funded by Grant-in-Aid for Scientific Research on Innovative Areas "Singularity Biology" (JP18H05410 to HY, JP18H05414 to HB) from the Ministry of Education, Culture, Sports, Science and Technology, Japan, JSPS Grants-in-Aid for Scientific Research JP20K06896, JP23K05993 to YS, JP21H02450, 23K18116 to HB, and grants from Naito foundation and Takeda Science Foundation to HB. DeepL, ChatGPT 3.5, Grammarly, and Enago the editing brand of Crimson Interactive Pvt. Ltd supported the English editing of this article.

This article is licensed under the Creative Commons Attribution-NonCommercial-ShareAlike 4.0 International License.
To view a copy of this license, visit https://creativecommons.org/licenses/by-nc-sa/4.0/.

## References


[1] Gotz, J., Halliday, G., Nisbet, R.M. Molecular pathogenesis of the tauopathies. Annu Rev Pathol 14, 239-261 (2019). https://doi.org/10.1146/annurev-pathmechdis-012418-012936

[2] Alquezar, C., Arya, S., Kao, A.W. Tau post-translational modifications: Dynamic transformers of tau function, degradation, and aggregation. Front Neurol 11, 595532 (2020). https://doi.org/10.3389/fneur.2020.595532

[3] Braak, H., Del Tredici, K. The pathological process underlying alzheimer's disease in individuals under thirty. Acta Neuropathol 121, 171-181 (2011). https://doi.org/10.1007/s00401-010-0789-4

[4] Braak, H., Thal, D.R., Ghebremedhin, E., Del Tredici, K. Stages of the pathologic process in alzheimer disease: Age categories from 1 to 100 years. J Neuropathol Exp Neurol 70, 960-969 (2011). https://doi.org/10.1097/NEN.0b013e318232a379

[5] Ossenkoppele, R., Schonhaut, D.R., Schöll, M., Lockhart, S.N., Ayakta, N., Baker, S.L., et al. Tau pet patterns mirror clinical and neuroanatomical variability in alzheimer's disease. Brain 139, 1551-1567 (2016). https://doi.org/10.1093/brain/aww027

[6] Cho, H., Choi, J.Y., Hwang, M.S., Kim, Y.J., Lee, H.M., Lee, H.S., et al. In vivo cortical spreading pattern of tau and amyloid in the alzheimer disease spectrum. Annals of Neurology 80, 247-258 (2016). https://doi.org/https://doi.org/10.1002/ana.24711

[7] Allen, B., Ingram, E., Takao, M., Smith, M.J., Jakes, R., Virdee, K., et al. Abundant tau filaments and nonapoptotic neurodegeneration in transgenic mice expressing human p301s tau protein. J Neurosci 22, 9340-9351 (2002). https://doi.org/10.1523/jneurosci.22-21-09340.2002

[8] Santacruz, K., Lewis, J., Spires, T., Paulson, J., Kotilinek, L., Ingelsson, M., et al. Tau suppression in a neurodegenerative mouse model improves memory function. Science 309, 476-481 (2005). https://doi.org/10.1126/science.1113694

[9] Yoshiyama, Y., Higuchi, M., Zhang, B., Huang, S.M., Iwata, N., Saido, T.C., et al. Synapse loss and microglial activation precede tangles in a p301s tauopathy mouse model. Neuron 53, 337-351 (2007). https://doi.org/10.1016/j.neuron.2007.01.010

[10] Sahara, N., Yanai, R. Limitations of human tau-expressing mouse models and novel approaches of mouse modeling for tauopathy. Front Neurosci 17, 1149761 (2023). https://doi.org/10.3389/fnins.2023.1149761

[11] Iba, M., Guo, J.L., McBride, J.D., Zhang, B., Trojanowski, J.Q., Lee, V.M. Synthetic tau fibrils mediate transmission of neurofibrillary tangles in a transgenic mouse model of alzheimer's-like tauopathy. J Neurosci 33, 1024-1037 (2013). https://doi.org/10.1523/jneurosci.2642-12.2013

[12] Clavaguera, F., Akatsu, H., Fraser, G., Crowther, R.A., Frank, S., Hench, J., et al. Brain homogenates from human tauopathies induce tau inclusions in mouse brain. Proc Natl Acad Sci U S A 110, 9535-9540 (2013). https://doi.org/10.1073/pnas.1301175110

[13] Bell, B.J., Malvankar, M.M., Tallon, C., Slusher, B.S. Sowing the seeds of discovery: Tau-propagation models of alzheimer's disease. ACS Chem Neurosci 11, 3499-3509 (2020). https://doi.org/10.1021/acschemneuro.0c00531

[14] Narasimhan, S., Guo, J.L., Changolkar, L., Stieber, A., McBride, J.D., Silva, L.V., et al. Pathological tau strains from human brains recapitulate the diversity of tauopathies in nontransgenic mouse brain. J Neurosci 37, 11406-11423 (2017). https://doi.org/10.1523/JNEUROSCI.1230-17.2017

[15] Vogels, T., Leuzy, A., Cicognola, C., Ashton, N.J., Smolek, T., Novak, M., et al. Propagation of tau pathology: Integrating insights from postmortem and in vivo studies. Biol Psychiatry 87, 808-818 (2020). https://doi.org/10.1016/j.biopsych.2019.09.019

[16] Calafate, S., Buist, A., Miskiewicz, K., Vijayan, V., Daneels, G., de Strooper, B., et al. Synaptic contacts enhance cell-to-cell tau pathology propagation. Cell Reports 11, 1176-1183 (2015). https://doi.org/https://doi.org/10.1016/j.celrep.2015.04.043

[17] Pérez, M., Avila, J., Hernández, F. Propagation of tau via extracellular vesicles. Frontiers in Neuroscience 13 (2019). https://doi.org/10.3389/fnins.2019.00698

[18] Nagai, T. Editorial: Singularity biology and beyond. Biophysics and Physicobiology advpub (2024). https://doi.org/10.2142/biophysico.bppb-v21.s013

[19] Ichimura, T., Kakizuka, T., Sato, Y., Fujioka, Y., Ohba, Y., Horikawa, K., et al. Strength in numbers: Unleashing the potential of trans-scale scope amateras for massive cell quantification. Biophysics and Physicobiology advpub (2024). https://doi.org/10.2142/biophysico.bppb-v21.s017

[20] Bannai, H., Takashima, A., Soeda, Y., Yoshimura, H., Matsumoto, G., Sahara, N., et al. Research on the molecular mechanism of singularity phenomenon in neurological disorders. Biophysics and Physicobiology advpub (2024). https://doi.org/10.2142/biophysico.bppb-v21.s008

[21] Taslimi, A., Vrana, J.D., Chen, D., Borinskaya, S., Mayer, B.J., Kennedy, M.J., et al. An optimized optogenetic clustering tool for probing protein interaction and function. Nat Commun 5, 4925 (2014).

https://doi.org/10.1038/ncomms5925

[22] Tiwari, P., Tolwinski, N.S. Using optogenetics to model cellular effects of alzheimer's disease. Int J Mol Sci 24 (2023). https://doi.org/10.3390/ijms24054300

[23] Zhang, X., Vigers, M., McCarty, J., Rauch, J.N., Fredrickson, G.H., Wilson, M.Z., et al. The proline-rich domain promotes tau liquid-liquid phase separation in cells. J Cell Biol 219 (2020). https://doi.org/10.1083/jcb.202006054

[24] Jiang, L., Lin, W., Zhang, C., Ash, P.E.A., Verma, M., Kwan, J., et al. Interaction of tau with hnrnpa2b1 and n(6)-methyladenosine rna mediates the progression of tauopathy. Mol Cell 81, 4209-4227 e4212 (2021). https://doi.org/10.1016/j.molcel.2021.07.038

[25] Soeda, Y., Yoshimura, H., Bannai, H., Koike, R., Takashima, A. Intracellular tau fragment droplets serve as seeds for tau fibrils. bioRxiv, 2023.2009.2010.557018 (2023). https://doi.org/10.1101/2023.09.10.557018

[26] Hiroshima, M., Bannai, H., Matsumoto, G., Ueda, M. Application of single-molecule analysis to singularity phenomenon of cells. Biophysics and Physicobiology advpub (2024). https://doi.org/10.2142/biophysico.bppb-v21.s018

[27] Guo, J.L., Narasimhan, S., Changolkar, L., He, Z., Stieber, A., Zhang, B., et al. Unique pathological tau conformers from alzheimer's brains transmit tau pathology in nontransgenic mice. J Exp Med 213, 2635-2654 (2016). https://doi.org/10.1084/jem.20160833

[28] Gyparaki, M.T., Arab, A., Sorokina, E.M., Santiago-Ruiz, A.N., Bohrer, C.H., Xiao, J., et al. Tau forms oligomeric complexes on microtubules that are distinct from tau aggregates. Proc Natl Acad Sci U S A 118 (2021). https://doi.org/10.1073/pnas.2021461118

[29] Guthrie, C.R., Kraemer, B.C. Proteasome inhibition drives hdac6-dependent recruitment of tau to aggresomes. J Mol Neurosci 45, 32-41 (2011). https://doi.org/10.1007/s12031-011-9502-x

[30] Santa-Maria, I., Varghese, M., Ksiezak-Reding, H., Dzhun, A., Wang, J., Pasinetti, G.M. Paired helical filaments from alzheimer disease brain induce intracellular accumulation of tau protein in aggresomes. J Biol Chem 287, 20522-20533 (2012). https://doi.org/10.1074/jbc.M111.323279

[31] Kopito, R.R. Aggresomes, inclusion bodies and protein aggregation. Trends Cell Biol 10, 524-530 (2000). https://doi.org/10.1016/s0962-8924(00)01852-3

[32] Kawaguchi, Y., Kovacs, J.J., McLaurin, A., Vance, J.M., Ito, A., Yao, T.-P. The deacetylase hdac6 regulates aggresome formation and cell viability in response to misfolded protein stress. Cell 115, 727-738 (2003). https://doi.org/https://doi.org/10.1016/S0092-8674(03)00939-5

[33] Jicha, G.A., Bowser, R., Kazam, I.G., Davies, P. Alz-50 and mc-1, a new monoclonal antibody raised to paired helical filaments, recognize conformational epitopes on recombinant tau. J Neurosci Res 48, 128-132 (1997). https://doi.org/10.1002/(sici)1097-4547(19970415)48:2<128::aid-jnr5>3.0.co;2-e

[34] Jicha, G.A., Lane, E., Vincent, I., Otvos, L., Jr., Hoffmann, R., Davies, P. A conformation- and phosphorylation-dependent antibody recognizing the paired helical filaments of alzheimer's disease. J Neurochem 69, 2087-2095 (1997). https://doi.org/10.1046/j.1471-4159.1997.69052087.x

[35] Ono, M., Komatsu, M., Ji, B., Takado, Y., Shimojo, M., Minamihisamatsu, T., et al. Central role for p62/sqstm1 in the elimination of toxic tau species in a mouse model of tauopathy. Aging Cell 21, e13615 (2022). https://doi.org/10.1111/acel.13615

[36] Horowitz, P.M., LaPointe, N., Guillozet-Bongaarts, A.L., Berry, R.W., Binder, L.I. N-terminal fragments of tau inhibit full-length tau polymerization in vitro. Biochemistry 45, 12859-12866 (2006). https://doi.org/10.1021/bi061325g

[37] Hosokawa, M., Masuda-Suzukake, M., Shitara, H., Shimozawa, A., Suzuki, G., Kondo, H., et al. Development of a novel tau propagation mouse model endogenously expressing 3 and 4 repeat tau isoforms. Brain 145, 349-361 (2021). https://doi.org/10.1093/brain/awab289